Aldose Reductases Influence Prostaglandin F2α Levels and Adipocyte Differentiation in Male Mouse and Human Species

Emilie Pastel, Jean-Christophe Pointud, Gaëlle Loubeau, Christian Dani, Karem Slim, Gwenaëlle Martin, Fanny Volat, Isabelle Sahut-Barnola, Pierre Val, Antoine Martinez, et al.

Aldose Reductases Influence Prostaglandin $F_{2\alpha}$ Levels and Adipocyte Differentiation in Male Mouse and Human Species

Emilie Pastel, Jean-Christophe Pointud, Gaëlle Loubeau, Christian Dani, Karem Slim, Gwenaëlle Martin, Fanny Volat, Isabelle Sahut-Barnola, Pierre Val, Antoine Martinez, and Anne-Marie Lefrançois-Martinez

Centre National de la Recherche Scientifique Unité Mixte de Recherche 6293 (E.P., J.-C.P., G.L., I.S.-B., P.V., A.M., A.-M.L.-M.), INSERM Unité 1103, Génétique Reproduction et Développement, Clermont Université, 63171 Aubière, France; iBV (C.D.), Institute of Biology Valrose, Université Nice Sophia Antipolis, 06189 Nice, France; Service de Chirurgie Digestive (K.S., G.M.), Centre Hospitalier Universitaire Estaing, 63003 Clermont-Ferrand, France; and INSERM Unité Mixte de Recherche 1048 (F.V.), Institute of Metabolic and Cardiovascular Diseases, Université Paul Sabatier, 31432 Toulouse, France

Aldose reductases (AKR1B) are widely expressed oxidoreductases whose physiological function remains elusive. Some isoforms are genuine prostaglandin $F_{2\alpha}$ ($PGF_{2\alpha}$) synthases, suggesting they might influence adipose homeostasis because $PGF_{2\alpha}$ inhibits adipogenesis. This was shown by *Akr1b7* gene ablation in the mouse, which resulted in increased adiposity related to a lower $PGF_{2\alpha}$ content in fat. Yet humans have no ortholog gene for *Akr1b7*, so the role of aldose reductases in human adipose homeostasis remains to be explored. We analyzed expression of genes encoding human and mouse aldose reductase isoforms in adipose tissues and differentiating adipocytes to assess conserved mechanisms regulating $PGF_{2\alpha}$ synthesis and adipogenesis. The *Akr1b3* gene encoded the most abundant isoform in mouse adipose tissue, whereas *Akr1b7* encoded the only isoform enriched in the stromal vascular fraction. Most mouse aldose reductase gene expression peaked in early adipogenesis of 3T3-L1 cells and diminished with differentiation. In contrast with its mouse ortholog *Akr1b3*, *AKR1B1* expression increased throughout differentiation of human multipotent adipose-derived stem cells, paralleling $PGF_{2\alpha}$ release, whereas $PGF_{2\alpha}$ receptor (FP) levels collapsed in early differentiation. Pharmacological inhibition of aldose reductase using Statil altered $PGF_{2\alpha}$ production and enhanced human multipotent adipose-derived stem adipocyte differentiation. As expected, the adipogenic effects of Statil were counteracted by an FP agonist (cloprostenol). Thus, in both species aldose reductase-dependent $PGF_{2\alpha}$ production could be important in early differentiation to restrict adipogenesis. $PGF_{2\alpha}$ antiadipogenic signaling could then be toned down through the FP receptor or aldose reductases down-regulation in human and mouse cells, respectively. Our data suggest that aldose reductase inhibitors could have obesogenic potential.

Abbreviations: AKR1B1, aldo-keto reductase family 1 member B1; AKR, aldo-keto reductase; aP2, adipose protein 2; BAT, brown adipose tissue; BMI, body mass index; C/EBPα, CCAAT/enhancer-binding protein α; COX, cyclooxygenase; CREB, cAMP-responsive element binding protein; Ct, cycle threshold; DMSO, dimethylsulfoxide; EIA, enzyme immunoassay; FABP4, fatty acid binding protein 4; FCS, fetal calf serum; FGF, fibroblast growth factor; FP, prostaglandin F receptor; gWAT, gonadal WAT; hMADS, human multipotent adipose-derived stem cell; iWAT, inguinal WAT; $PGF_{2\alpha}$, prostaglandin $F_{2\alpha}$; PPARγ, peroxisome proliferator-activated receptor-γ; PTGFR, prostaglandin F receptor gene; Rald, retinaldehyde; RT-qPCR, real-time quantitative PCR; rWAT, retroperitoneal WAT; SVF, stromal vascular fraction; WAT, white adipose tissue; Zfp521/ZNF521, zinc finger protein 521.

Aldose reductases (AKR1B; Enzyme Classification 1.1.1.21) are cytosolic monomeric enzymes belonging to the aldo-keto reductase (AKR) superfamily that reduce aldehyde or ketone function into corresponding alcohol from various aliphatic or aromatic substrates. This superfamily encompasses more than 150 nicotinamide adenine dinucleotide (phosphate)(reduced)-dependent oxidoreductases distributed in all prokaryotic and eukaryotic kingdoms. In humans, three distinct aldose reductase isoforms encoded by three different genes have been characterized so far: *AKR1B1* [human aldose reductase (AR); (1)], *AKR1B10* [also designated as human small intestine reductase or aldose reductase-like-1) (2, 3)]; and *AKR1B15* (4). Four mouse aldose reductase isoforms have been described: Akr1b3, also referred to as murine aldose reductase is encoded by the ortholog gene of *AKR1B1* (5); Akr1b7 [previously named mouse vas deferens protein (6)]; Akr1b8, encoded by the ortholog gene of *AKR1B10* [previously named fibroblast growth factor (FGF)-related protein 1 (7)]; and Akr1b16 (4).

Aldose reductases belong to one of the most characterized AKR subgroups. Indeed, human aldose reductase-B1 is notoriously associated with diabetic complications, resulting from its ability to reduce glucose into sorbitol in a nicotinamide adenine dinucleotide phosphate reduced+H^+-dependent manner, which promotes osmotic and oxidative stresses. In addition to glucose conversion, human and murine aldose reductases display reductase activities for various substrates including aldehydes, retinoids, xenobiotics, and prostaglandins (PG). This wide range of substrates allows them to participate in many pathological processes related to diabetes, tumorigenesis (8–12), or inflammation (13–18). This has prompted the development of specific aldose reductase inhibitors for targeting these pathological manifestations, but their physiological function still remains elusive (19).

Activation of biological pathways that favor adipocyte differentiation from precursor cells results in an increase in the number of adipocytes that may be critical for overall metabolic balance. Therefore, adipocyte expansion is tightly regulated by factors promoting or inhibiting adipocyte development. Among paracrine/autocrine factors produced by white adipose tissue (WAT), $PGF_{2\alpha}$ acting through the prostaglandin F receptor (FP) coupled to MAPK and/or Ca^{2+} signaling was previously shown to suppress adipocyte differentiation by inhibiting the function/expression of the critical proadipogenic transcription factor peroxisome proliferator-activated receptor-γ (PPARγ) and CCAAT/enhancer-binding protein-α (C/EBPα) (20, 21).

We and others previously showed that mammalian aldose reductase isoforms can be distinguished according to their ability to produce $PGF_{2\alpha}$ through the reduction of the 9-,11-endoperoxide moiety of the common prostaglandin precursor PGH_2, supplied by cyclooxygenases COX-1 or COX-2 (16, 22). Human aldose reductase-B1 and mouse-b3 and -b7 were shown to possess this $PGF_{2\alpha}$ synthase activity, whereas aldose reductase-B10 and mouse-b8 isoforms were devoid of it (22). We recently reported that mice deficient for *Akr1b7* displayed excessive basal adiposity, resulting from both adipocyte hyperplasia and hypertrophy under a normal diet and in the absence of increased food intake. Aldose reductase-b7 loss was associated with decreased $PGF_{2\alpha}$ levels in WAT. Moreover, cloprostenol ($PGF_{2\alpha}$ analog) administration in *Akr1b7*$^{-/-}$ mice normalized WAT expansion by altering both de novo adipocyte differentiation and size (23), suggesting that this isoform was an important regulator of WAT homeostasis through $PGF_{2\alpha}$-dependent mechanisms (23). Another isoform was proposed to fulfill anti-adipogenic function in the mouse. Indeed, $PGF_{2\alpha}$ produced by aldose reductase-b3 was shown to suppress adipocyte differentiation in the mouse 3T3-L1 cell line (24). Yet the absence of an adipose phenotype in *Akr1b3*-deficient mice suggested that redundant functions from other isoforms might compensate for the lack of aldose reductase-b3 in vivo (25). Conversely, some specific expression properties of the b7 isoform could explain its nonredundant function as evidenced by the increased adiposity of *Akr1b7*-deficient mice. Humans have no direct ortholog genes for *Akr1b7*. Although aldose reductase-B1 was recently shown to be expressed in human subcutaneous adipose tissue (26), its contribution to WAT homeostasis was not established.

The aim of the present study was to provide quantification of mouse and human aldose reductase isoforms in adipose depots and during adipocyte differentiation in culture to explore conserved mechanisms regulating $PGF_{2\alpha}$ synthesis and to evaluate involvement of human aldose reductases in $PGF_{2\alpha}$-mediated regulation of WAT homeostasis. We show herein that murine isoforms present specific expression patterns in adipose tissue/cells and that human aldose reductase could influence adipogenesis in a $PGF_{2\alpha}$-dependent manner that can be pharmacologically modulated.

Materials and Methods

Biological materials

129/sv mice were housed in a room-controlled temperature with 12-hour light, 12-hour dark cycles in agreement with international standards for animal welfare. They were fed ad libitum with water and a Global diet (Harlan). Four- to 6-month-old male mice were killed by cervical dislocation, and different tissues, including fat pads from various locations were removed

and immediately frozen in liquid nitrogen and stored at −80°C until use.

Human adipose tissues specimens (sc fat) were obtained from seven subjects who were undergoing abdominal surgery at Estaing Hospital, Clermont-Ferrand (Auvergne, France). They were aged between 28 and 61 years with a body mass index (BMI) higher than 25 kg/m^2. These samples were immediately frozen in liquid nitrogen. The hospital's Ethics Committee approved this study.

Adipose tissue fractionation

Murine fat pads freshly excised were rinsed in Krebs-Ringer bicarbonate buffer, minced, and digested for 30 minutes at 37°C in DMEM (Invitrogen) containing 1 g/L of type II collagenase (Sigma-Aldrich). Undigested tissues were removed by filtration through a 250-μm nylon sieve. After centrifugation of the filtrate at 750 × *g* for 10 minutes, the floating adipocyte fraction was separated from the stromal vascular pellet, and each fraction was stored at −80°C until use.

Cell culture and treatment

Mouse 3T3-L1 preadipocytes were cultured, and differentiation was induced as previously described (27). Briefly, for the amplification step, cells were cultured in DMEM (Invitrogen) supplemented with 10% of bovine serum (Biowest), 2 mM L-glutamine, 100 U/mL penicillin, and 0.1 mg/mL streptomycin (Invitrogen) at 37°C in a humidified atmosphere with 5% CO_2. Then 80 000 plated cells/cm^2 were cultured in DMEM supplemented with fetal calf serum (FCS). Adipocyte differentiation of confluent 3T3-L1 cells was initiated with DMEM supplemented with 10% FCS, 500 nM dexamethasone, 0.1 μM insulin, and 500 μM isobutylmethylxanthine (Sigma-Aldrich).

After 48 hours, the culture medium was replaced with DMEM containing 10% FCS and 0.1 μM insulin. From the fifth day, cells were cultured with DMEM supplemented with 10% FCS until complete adipocyte differentiation. Human multipotent adipose-derived stem (hMADS)-3 cells were cultured and differentiated as previously described (28, 29). hMADS cells were routinely maintained in proliferation in DMEM (Lonza) containing 10% FCS, 2 mM L-glutamine, 100 U/mL penicillin, and 0.1 mg/mL streptomycin at 37°C in a humidified atmosphere with 5% CO_2. Cells were plated at 40 000 cells/cm^2 in growth medium containing 2.5 ng/mL FGF2 (Peprotech). Two days after seeding, FGF2 was removed from proliferation medium. On the next day, differentiation of confluent cells was induced with DMEM/Ham's F12 (Lonza) supplemented with 0.86 μM insulin, 10 μg/mL transferrin, 1 μM dexamethasone, 100 μM isobutylmethylxanthine, 1 μM rosiglitazone, and 0.2 nM triiodothyronine (Sigma-Aldrich). At day 3, dexamethasone and isobutylmethylxanthine were removed. To evaluate the involvement of aldose reductases during adipogenesis, some hMADS cell batches were differentiated in the presence of either the aldose reductase inhibitor Statil, 1–10 μM (Santa Cruz Biotechnology), or dimethylsulfoxide (DMSO; vehicle) or in combination with 0.1 μM cloprostenol for various amounts of time as indicated in the figure legends. Cells were then harvested for further analysis.

Cell line authentication

3T3-L1 cell authenticity has been attested herein (see Figure 2) by analyzing their adipogenesis in real-time quantitative PCR (RT-qPCR) analyses using mouse specific primers for adipogenic genes and Oil-Red-O staining. hMADS-3 cell authenticity has been performed recently via analyzing their immunophenotype and their adipogenesis [see Supplemental Table 2 and Figure 2, respectively, of the report of Mohsen et al (30)].

Oil-Red-O staining

hMADS cells were fixed in 4% paraformaldehyde and stained with Oil-Red-O (Sigma-Aldrich) as previously described (31). Measurement by spectrophotometry of Oil-Red-O staining was performed by dissolving the intracellular lipid droplets with isopropanol. Absorbance was measured at 490 nm.

Gene expression

Total RNA were extracted from human and mouse tissues or hMADS or 3T3-L1 cells using TRI reagent (Molecular Research Center, Inc). RNA concentration and purity were assessed spectrophotometrically using a NanoDrop 1000 (Thermo Scientific). One microgram of mRNA was reverse transcribed for 1 hour at 37°C with 5 pmol of random hexamer primers, 200 U of Moloney murine leukemia virus-reverse transcriptase (Promega), 2 mM deoxynucleotide triphosphates, and 20 U of RNAsin (Promega). Two microliters of a fifth dilution of cDNA were used in each PCR.

RT-qPCR was performed on a Mastercycler ep Realplex (Eppendorf) using MESA GREEN quantitative PCR master mix Plus for SYBR (Eurogentec). Amplification was performed as follows: initial denaturation at 95°C for 2 minutes, followed by 40 cycles of 94°C for 15 seconds, 60°C for 15 seconds, 72°C for 20 seconds. The specificity of each reaction was determined after completion of PCR cycling by analysis of the melting point dissociation curve generated for temperatures from 60°C to 95°C at 0.2°C/s. Each reaction was performed in duplicate for each sample and relative expression was calculated based on the standard curve method normalized to *TBP* for hMADS cells and *Ppib* for 3T3-L1 cells (see Supplemental Table 1 for primer sequence). Amplification efficiency was determined for each pair of primers and a 100% ± 5% efficiency conditioned their use in quantitative PCR analyses.

Murine aldose reductases mRNA absolute quantification was performed in various tissues following the method of Pfaffl (32). Briefly, cDNA of each aldose reductase and *18S* RNA was cloned in a pGEM-T Easy Vector (Promega) and then was sequenced (GATC Biotech) to confirm the correct insertion of cDNA in plasmid. After mRNA reverse transcription, aldose reductase cDNAs resulting products were quantified by quantitative PCR using calibration curves with known concentrations of plasmid DNA between 10^{-2} and 10^{-7} ng. Potential RNA quantity variations between tissue extracts were corrected with *18S* RNA quantification (see Supplemental Table 2 for primer sequences). Results were expressed as femtomole of aldose reductase mRNA per microgram of total RNA.

For semiquantitative RT-PCR experiments, PCRs were performed by using GoTaq polymerase (Promega). PCR conditions were as follows: 5 minutes at 94°C followed by 22–33 cycles of 45 seconds at 94°C, 45 seconds at the optimal annealing temperature determined by gradient PCR (*Actin*, 22 cycles, 60°C;

Acc, 25 cycles, 65°C; *Zfp521*, 27 cycles, 65°C; *Akr1b3* 27 cycles, 65°C; *Akr1b7*, 33 cycles, 69°C; *Akr1b8*, 30 cycles, 69°C; *Akr1b16*, 30 cycles, 65°C), and 30 seconds at 72°C with a final elongation step of 5 minutes at 72°C (Supplemental Table 1). Aliquots of PCR products were analyzed on a 2% ethidium bromide-stained agarose gel and signals were quantified with Multi Gauge Software suite (Fujifilm).

Western blot

Cellular and tissue samples were homogenized in cold extraction buffer containing 20 mM HEPES, 0.42 M NaCl, 1.5 mM $MgCl_2$, 0.2 mM EDTA, 2 mM NaF, 2 mM Na_3VO_4, and protease inhibitors cocktail (Complete protease inhibitor cocktail tablets; Roche Diagnostics). After centrifugation at 4°C for 15 minutes at 13 000 rpm, concentration of soluble proteins was determined by the Bradford method (Bio-Rad Laboratories). Fifty micrograms of total proteins were subjected to a denaturing SDS-PAGE and electrotransferred onto Hybond-ECL membrane (GE Healthcare). Detections were performed using primary antibodies (Table 1) raised against FP receptor (1:500; Cayman Chemical) human COX-1 (1:500; Santa Cruz Biotechnology), murine COX-1 (1:500; Cayman Chemical), COX-2 (1:1000; Cayman Chemical), AKR1B1 and AKR1B10 (1:1000, kind gifts of Dr D. Cao, Department of Medical Microbiology, Immunology, and Cell Biology, Simmons Cancer Institute, SIU School of Medicine, Springfield, Illinois), FABP4 (1:500; R&D Systems), Akr1b3 (1:2000, L5), Akr1b7 (1:3000, L4), Akr1b8 (1:1000, L8) (33), α-tubulin (1:20 000; Sigma-Aldrich) and revealed with a peroxidase-conjugate antirabbit, antimouse, antigoat, or antirat secondary antibody (Production d'Anticorps, Réactifs Immunologiques and Services). Detection was performed using Immobilon Western chemiluminescent horseradish peroxidase substrate (Millipore), and signals were quantified with a DNR MF ChemiBis 3.2 camera and Multi Gauge Software suite (Fujifilm).

$PGF_{2\alpha}$ dosage

Culture media samples were collected every 72 hours, immediately frozen in liquid nitrogen, and stored at −80°C. $PGF_{2\alpha}$ released in culture media was measured by an enzyme immunoassay (EIA) and acetylcholinesterase-linked $PGF_{2\alpha}$ tracer (Cayman Chemical) according to the manufacturer's instructions.

Statistical analyses

Results were expressed as means ± SD (or SEM when indicated). Statistical significance of differences between experimental groups was assessed using tests specified in the figure legends. All tests were performed using GraphPad Prism 5 (GraphPad Software).

Results

Comparative tissue expression of mouse aldose reductase genes

mRNA expression levels of the four mouse genes (*Akr1b3*, *b7*, *b8*, *b16*) were measured by RT-qPCR absolute quantification in a set of 15 tissues. PCR was performed using specific primers that target the most divergent part of the transcripts encompassing the 17 C-terminal amino acids encoding sequences and the 3′-

Table 1. Antibody Table

Peptide/ Protein Target	Antigen Sequence (if Known)	Name of Antibody	Manufacturer, Catalog Number, and/or Name of Individual Providing the Antibody	Species Raised (Monoclonal or Polyclonal)	Dilution Used
FP receptor	SMNSSKQPVSPAAGL	FP receptor polyclonal antibody	Cayman Chemical; number 101802	Rabbit; polyclonal	1:500
Human COX-1		Cox-1 (C-20): sc-1752	Santa Cruz Biotechnology; number sc-1752	Goat; polyclonal	1:500
Mouse COX-1	LMRYPPGVPPERQMA	COX-1 (murine) polyclonal antibody	Cayman Chemical; number 160109	Rabbit; polyclonal	1:500
COX-2	DPQPTKTATINASASHS RLDDINPTVLIK	COX-2 (murine) polyclonal antibody	Cayman Chemical; number 160106	Rabbit; polyclonal	1:1000
AKR1B1			Dr Deliang Cao	Rabbit; polyclonal	1:1000
AKR1B10			Dr Deliang Cao	Rabbit; polyclonal	1:1000
FABP4			R&D Systems; number MAB1443	Rat; monoclonal	1:500
Akr1b3	ALMSCAKHKDYPFHAEV	L5	Professor Anne-Marie Lefrançois-Martinez	Rabbit; polyclonal	1:2000
Akr1b7	DLLDARTEEDYPFHEEY	L4	Professor Anne-Marie Lefrançois-Martinez	Rabbit; polyclonal	1:1000
Akr1b8	LLPETVNMEEYPYDAEY	L8	Professor Anne-Marie Lefrançois-Martinez	Rabbit; polyclonal	1:3000
α-Tubulin		Monoclonal anti-α-tubulin antibody	Sigma-Aldrich; number T6074	Mouse; monoclonal	1:20 000

Table 2. Absolute Quantification of mRNA for Akr1b Isoforms in Mouse Tissues

	$\times 10^{-9}$ fmol/μg^{-1} of Total RNA			
	Akr1b3	***Akr1b7***	***Akr1b8***	***Akr1b16***
gWAT	7.04 ± 1.38	**1.78 ± 1.55[3]**	**1.32 ± 0.44[3]**	**0.80 ± 0.32[5]**
iWAT	2.40 ± 0.55	0.08 ± 0.05	0.55 ± 0.29	0.28 ± 0.14
rWAT	1.96 ± 0.51[a]	0.08 ± 0.02	**0.86 ± 0.38[5]**	0.66 ± 0.33
BAT	8.34 ± 2.17	0.01 ± 0.002	0.73 ± 0.15	**0.88 ± 0.05[4]**
Testis	**31.86 ± 4.19[1a]**	**0.35 ± 0.05[5]**	**4.68 ± 0.49[1a]**	0.33 ± 0.19
Intestine	7.47 ± 4.20	**0.52 ± 0.08[4]**	0.26 ± 0.16	0.08 ± 0.07
Kidney	**27.65 ± 3.91[2]**	0.16 ± 0.01	0.22 ± 0.08	**1.23 ± 0.55[3]**
Adrenal	**17.61 ± 2.22[3]**	**311.93 ± 46.93[2]**	**3.95 ± 0.71[2]**	**6.94 ± 1.13[1a]**
Spleen	3.60 ± 0.26	0.16 ± 0.06	0.12 ± 0.07	0.03 ± 0.004
Liver	**14.80 ± 3.27[4]**	0.15 ± 0.07	0.05 ± 0.02	0.02 ± 0.004[a]
Vas deferens	4.47 ± 0.51	**3994.30 ± 149.66[1a]**	0.27 ± 0.06	**2.51 ± 0.53[2]**
Lung	2.70 ± 0.15	0.01 ± 0.001[a]	0.31 ± 0.03	0.20 ± 0.02
Brain	**10.58 ± 3.00[5]**	0.03 ± 0.01	0.09 ± 0.04	0.72 ± 0.13
Muscle	2.53 ± 1.18	0.05 ± 0.01	0.03 ± 0.01[a]	0.35 ± 0.02
Heart	6.65 ± 1.17	0.03 ± 0.02	**1.00 ± 0.08[4]**	0.75 ± 0.21

RT-qPCR analyses were performed using total RNA from a set of 15 tissues (n = 4–9) from 4-month-old male mice. Each isoform level was expressed as femtomoles of the targeted mRNA in 1 μg of total RNA ± SEM. The top 5 expression sites for each *Akr1b* are in bold, and ranking is numbered on the right.

[a] Highest and lowest expression sites for each Akr1b gene.

untranslated region (Supplemental Figure 1). Overall, *Akr1b3* had the widest expression, with levels ranging from 1.96 to 31.86 $\times$ 10^{-9} fmol/μg^{-1} of total RNA in retroperitoneal WAT (rWAT) and testis, respectively (Table 2 and Supplemental Figure 2). It was also the major isoform in all the 15 examined organs except for vas deferens and adrenal. On the contrary, *Akr1b7* showed very high expression levels but only in a restricted number of tissues. Its expression culminated in vas deferens and adrenal (25 000 and 2000 times more than in other tissues, respectively). Secondary expression sites for the *Akr1b7* were gonadal WAT (gWAT), intestine, and testis (1.78, 0.52, and 0.35 $\times$ 10^{-9}fmol/μg^{-1} of total RNA, respectively). *Akr1b8* had rather low expression levels except in the adrenal and testis (3.95 and 4.68 $\times$ 10^{-9}fmol/μg^{-1} of total RNA, respectively). *Akr1b16* mRNA highest levels were observed in the adrenal (6.94 $\times$ 10^{-9}fmol/μg^{-1} of total RNA) but were low in vas deferens (2.51 $\times$ 10^{-9}fmol/μg^{-1} of total RNA) and in kidney (1.23 $\times$ 10^{-9} fmol/μg^{-1} of total RNA). Altogether these data indicated that the adrenal gland was a major common expression site for mouse aldose reductase genes.

In the present quantitative analysis, although brown adipose tissue (BAT) and WAT expressed low mRNA levels of aldose reductase genes, *Akr1b3* was still the predominantly expressed member (seven times more than other members), whereas *Akr1b8* and *Akr1b16* genes were expressed at lower levels (0.86 and 0.65 $\times$ 10^{-9} fmol/μg^{-1} of total RNA, respectively) (Table 2). *Akr1b7* showed a somewhat unique expression pattern characterized by detectable expression in gWAT and almost undetectable expression in BAT, inguinal WAT (iWAT), and rWAT. This suggested that fat pad-specific mechanisms could modulate its expression in adipose tissues.

Differential expression of aldose reductase genes in adipose fractions

To further characterize aldose reductase genes expression in adipose tissues, we performed cell tissue fractionations. In these experiments, WAT is fractionated into two different cell populations: adipocytes and a heterogeneous population collected in the stromal vascular fraction (SVF) encompassing undifferentiated precursors, macrophages, fibroblasts, leukocytes, epithelial, endothelial, and vascular cells (34). Detection of adipocyte acetyl-coenzyme A carboxylase (*Acc*) and progenitors-enriched zinc finger protein 521 (*Zfp521*) allowed confirmation of the quality of tissue fractionation (Figure 1, A–C). In all WAT depots, *Akr1b3* expression was detected in both adipocyte and SVF fractions with at least a 2-fold enrichment in adipocytes. In all depots, *Akr1b8* and *Akr1b16* were expressed similarly in both fractions except for rWAT in which *Akr1b16* mRNA was enriched 1.8-fold in mature adipocytes. Thus, expression of *Akr1b3*, *b8* and *b16* was detected in both mature adipocytes and in the adipocyte progenitor/precursor-containing SVF. In contrast, *Akr1b7* transcripts were absent from adipocytes fraction but were enriched in the SVF from gWAT. Differential expression of aldose reductase-b3 and -b7 (members endowed with $PGF_{2\alpha}$ synthase activity) was confirmed by Western blot analysis of adipose tissue fractions

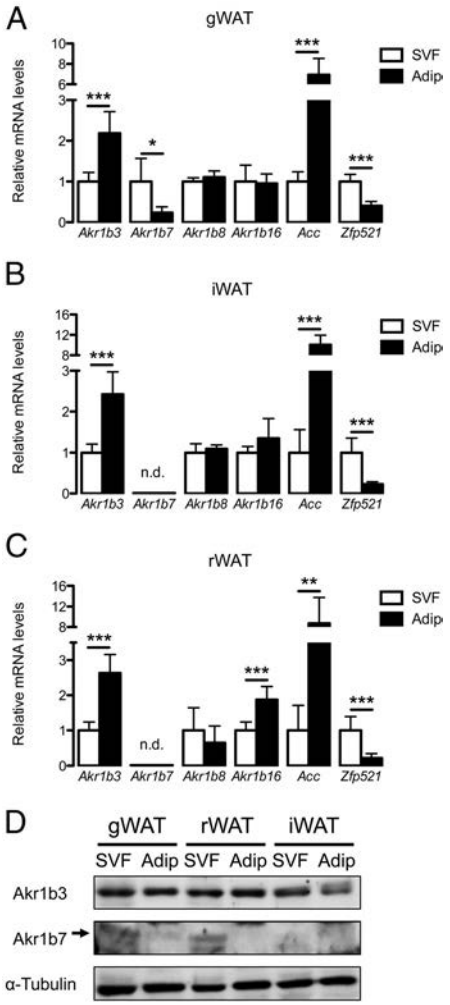

Figure 1. Differential expression of aldose reductase genes in stromal vascular and adipocyte fractions. Aldose reductase relative mRNA expression was evaluated by RT-PCR after tissue fractionation of gWAT, iWAT, and rWAT depots. A–C, Quantifications of RT-PCR signals. RT-PCR analyses were conducted using four independent RNA pools, each resulting from the fractionation of two to six fat pads. Signal intensity was quantified for each PCR product and normalized according to an *Actin* signal. For each gene, the mRNA level was expressed relative to the signal obtained for SVF, which was given the value 1. n.d., not detected. Statistical analyses were performed to compare expression of each gene in SVF and adipocyte fraction by unpaired *t* test. *, $P < .05$; **, $P < .01$; ***, $P < .001$. D, Akr1b3 and Akr1b7 proteins were monitored by Western blot on extracts from SVF and adipocyte fraction. α-Tubulin was used as a loading control.

(Figure 1D). Altogether these data showed coexpression of most genes encoding aldose reductase isoforms in both WAT cellular fractions, whereas *Akr1b7* was the only member of the subfamily to be exclusively expressed in SVF.

Differential expression of murine aldose reductase genes during adipogenesis in 3T3-L1 cells

Progenitor cells from SVF constitute a reservoir for adipose tissue maintenance when committed into an adipocyte fate. The mouse preadipocyte 3T3-L1 cell line is a well-characterized and widely used in vitro model to study adipocyte differentiation. To compare mouse aldose reductases expression during adipogenesis, 3T3-L1 differentiation was induced over a 2-week period. RT-qPCR analyses showed increased expression of *Fabp4* and *Pparγ* genes in 3T3-L1 cells at differentiation days 3 and 6, confirming adipocyte differentiation also attested by triglyceride accumulation using Oil-Red-O staining (Figure 2). In comparison with *Akr1b3*, *b8*, or *b16*, the *Akr1b7* gene was expressed at very low levels in 3T3-L1 cells (detection threshold quantitative PCR cycle threshold (Ct) values at approximately 33 for *Akr1b7* mRNA vs 22–28 for the other isoforms) (Figure 2A). Whereas *Akr1b16* expression was unaltered throughout the culture period, *Akr1b3*, *b7*, and *b8* mRNA levels increased from the onset of the adipogenic program (2.7-, 6-, and 2-fold, respectively) at differentiation day 3 and then progressively returned to basal expression levels found in undifferentiated cells. PGF receptor gene *(Ptgfr)* mRNA levels (encoding the FP receptor) underwent a transient increase (4-fold) at differentiation day 3, paralleling *Akr1b3*, *b7*, and *b8* expression patterns (Figure 2A). Moreover, aldose reductase-b3, -b7, -b8, and FP protein levels evaluated by Western blot paralleled their mRNA (Figure 2B). Finally, as previously shown (35, 36), we confirmed that COX-1 protein was constitutively expressed throughout the differentiation program, whereas COX-2 was acutely down-regulated from day 3 onward. We concluded that with the exception of *Akr1b16*, *Akr1b3*, *b7*, and *b8*, expression levels were all transiently increased during the early steps of adipogenesis with maximal expression at day 3 (at the onset of differentiation) and thereafter decreased during adipogenesis.

Differential expression of human aldose reductases during adipogenesis in hMADS cells

Involvement of human aldose reductases in adipose tissue homeostasis is poorly documented. Recent data reported a positive correlation between $PGF_{2\alpha}$ release in human preadipocytes isolated from obese women, BMI, and cytokine-induced *AKR1B1* expression (26). In contrast, the expression of the *AKR1B10* gene as well as that of *AKR1C3* and *AKR1A1*, two genes encoding enzymes (3α-hydroxysteroid dehydrogenase type II and aldehyde reductase, respectively) with known PGF synthase activity, has never been studied in fat cells (37, 38). We also monitored the mRNA levels for COX-2 (*PTGS2* gene) and FP_A/FP_B receptors (*PTGFR1/PTGFR2* genes). RT-qPCR analyses showed no correlation between BMI and expression of these genes (Supplemental Figure 3). Western blot using specific antibodies (39) and RT-qPCR analyses con-

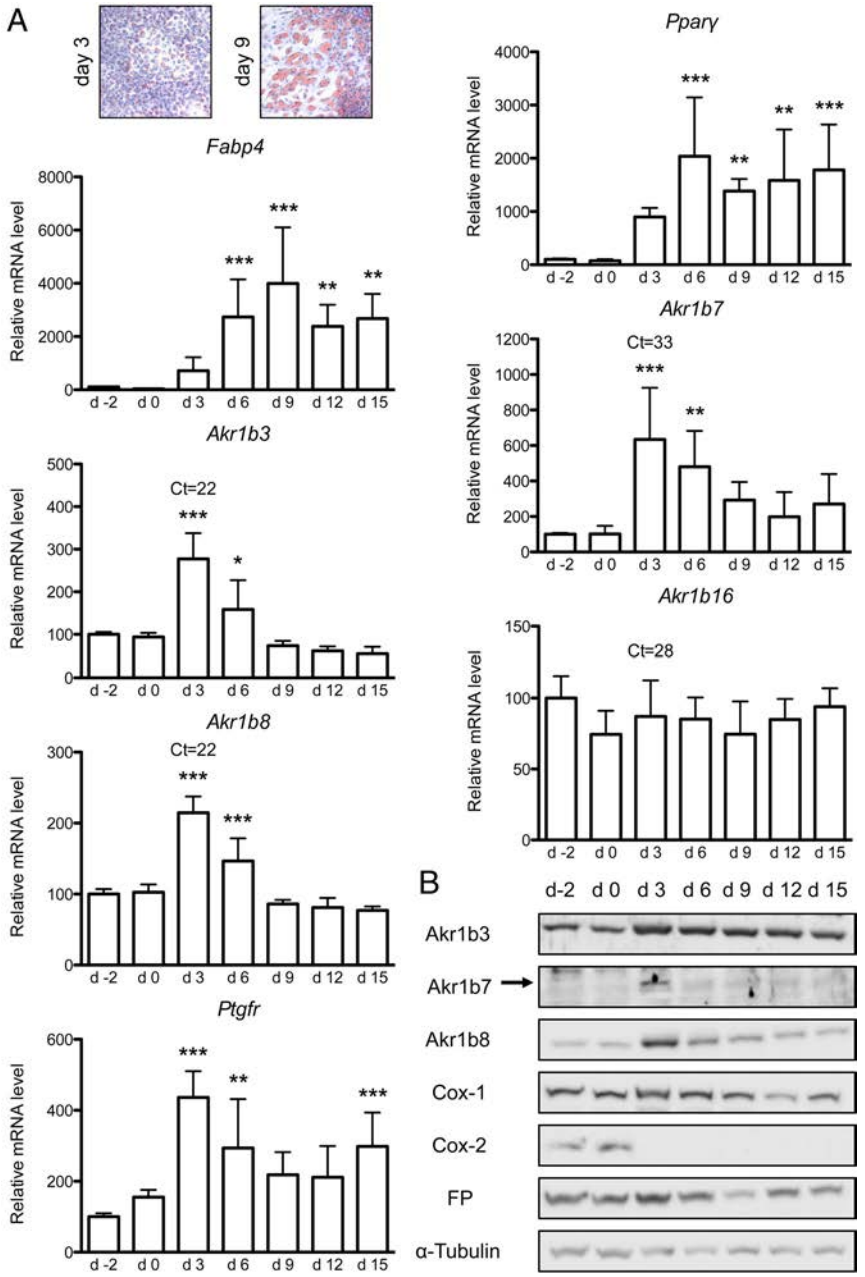

Figure 2. *Akr1b3*, *Akr1b7* and *Akr1b8* expression levels are transiently increased during the earlier step of 3T3-L1 adipogenesis. At day 0 (d0), 3T3-L1 preadipocytes were induced to differentiate into adipocytes (inset, Oil-Red-O staining showing progression of adipocyte differentiation of 3T3-L1 cells at days 3 and 9). A, From day 2 to day 15 of culture, mRNA levels of *Fabp4*, *Pparγ*, *Ptgfr*, *Akr1b3*, *Akr1b7*, *Akr1b8*, and *Akr1b16* were measured by RT-qPCR and normalized to *Ppib*. The qPCR Ct values from day 3 are indicated to compare relative expression level of the different *Akr1b* genes. mRNA quantifications were expressed as percentage of day 2 values. Statistical analyses were performed by one-way ANOVA followed by a Dunnett's post hoc test. *, $P < .05$; **, $P < .01$; ***, $P < .001$. B, Akr1b3, Akr1b8, Cox-1, Cox-2, and FP protein accumulations were monitored by Western blot throughout 3T3-L1 differentiation. α-Tubulin was used as a loading control.

firmed *AKR1B1* expression in intact sc WAT from obese patients, but no correlation with BMI was shown in our study. The discrepancy with data from Michaud et al (26) could result from the small size of our cohort. Although *AKR1B10* transcripts were detected in rather low amounts (average Ct 29.4), the protein remained undetectable in these WAT samples. This suggests that *AKR1B10* expression could either be absent or restricted to a minor population within sc WAT.

To analyze the expression of human aldose reductase isoforms during adipogenesis, we used a hMADS cell line that can be differentiated into functional adipocytes under adipogenic culture conditions (40). Adipogenesis was monitored by measuring changes at mRNA or protein levels of markers of the predifferentiation state (*ZNF521*, a regulator of adipose commitment ortholog to murine *Zfp521*) and early (*PPARγ*) and late (*LEPTIN*, *FABP4/aP2*) differentiation (Figure 3B and Supplemental Figure 4A). In agreement with progressive adipogenic differentiation, *PPARγ* mRNA expression increased from day 3 to reach a plateau between day 9 and day 12. As previously described in other preadipocyte lines, a 1.5-fold increase in the *ZNF521* mRNA level was transiently observed at day 0 in hMADS cells (41). Consistent with previous reports on leptin production, the highest *LEPTIN* mRNA level observed at day 6 was decreased 2-fold at day 9 (40). In agreement with full maturation of hMADS adipocytes, fatty acid binding protein 4 (FABP4)/adipose protein 2 (aP2) protein began to accumulate on day 9 (Supplemental Figure 4A). The lowest expression of *AKR1B1* mRNA was observed at day 3 and progressively increased to reach 210% of basal level at day 15 (Figure 3A). This expression time course was tightly correlated with changes in aldose reductase-B1 protein accumulation (Supplemental Figure 4A). In contrast, *AKR1B10* mRNA levels had their highest expression at day 0 and gradually decreased below 11% of the basal level throughout differentiation (Figure 3A). Unlike *AKR1B1* and *AKR1B10*, *AKR1A1* expression was only slightly and transiently increased (1.6-fold) between

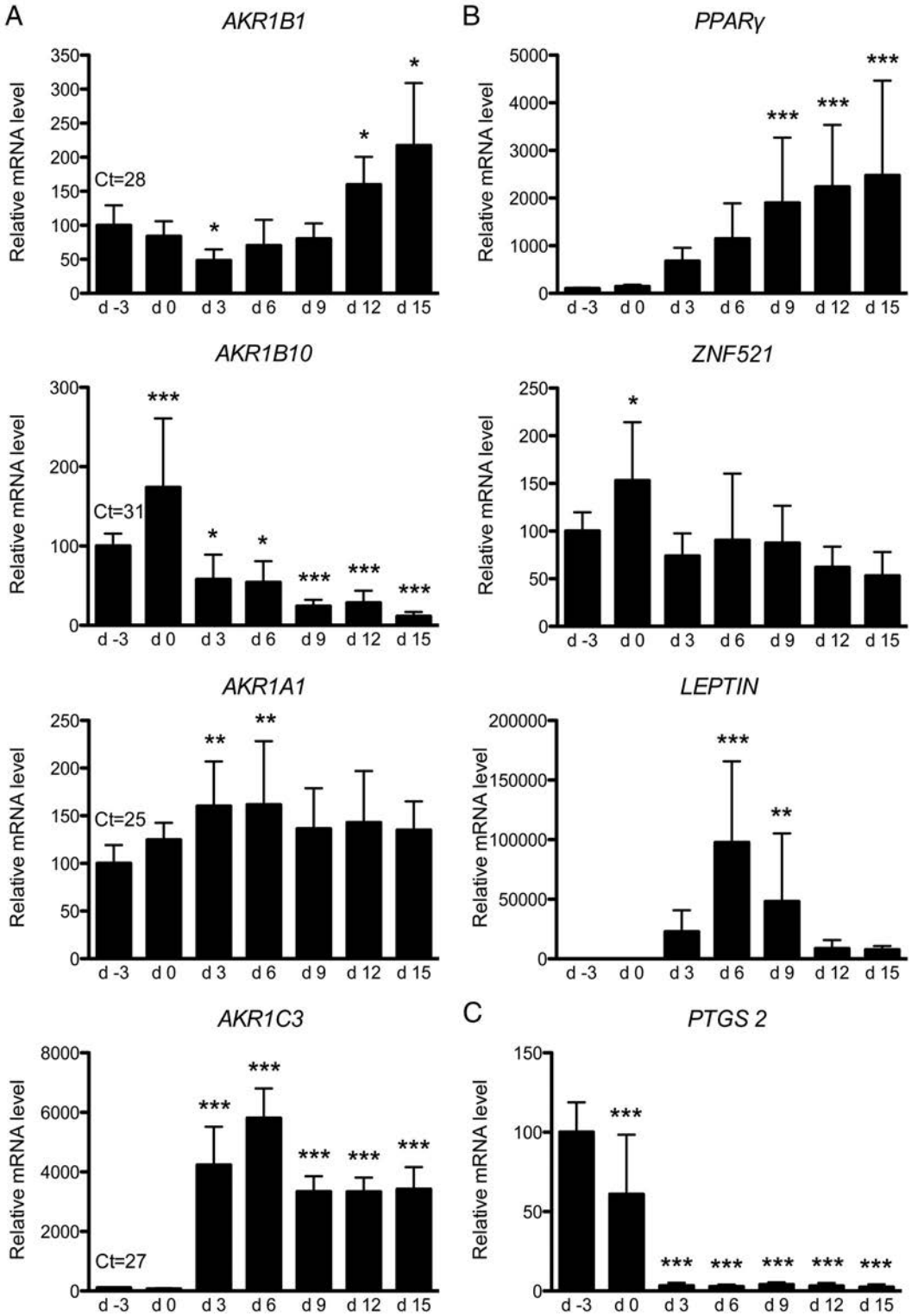

Figure 3. *AKR1B1* and *AKR1B10* display opposite expression profiles during hMADS cell adipogenesis. At day 0 (d0), hMADS preadipocytes were induced to differentiate into adipocytes. A, *AKR1B1*, *AKR1B10*, *AKR1A1*, and *AKR1C3* mRNA levels were measured by RT-qPCR throughout adipogenesis and values were normalized to *TBP*. B, To validate and follow the progress of adipogenic program, *PPARγ*, *ZNF521*, and *LEPTIN* gene expressions were analyzed by RT-qPCR and values were normalized to *TBP*. C, Level of *PTGS2* transcripts were measured by RT-qPCR and normalized to *TBP*. mRNA quantifications were expressed as a percentage of day 3 values. Statistical analyses were performed by one-way ANOVA followed by a Dunnett's post hoc test, each value was compared with day 3 value. *, $P < .05$; **, $P < .01$; ***, $P < .001$.

differentiation day 3 and day 6. mRNA level for *AKR1C3* was strongly induced (58-fold) from day 3 onward. Finally, COX-2 expression (*PTGS 2* gene) was high in preadipocytes and rapidly turned off after the onset of adipogenesis between day 0 and day 3 (Figure 3C). Taken together, these data suggested that *AKR1B10* and *AKR1B1* expression could be differentially involved in adipogenesis.

Aldose reductase-mediated $PGF_{2\alpha}$ release during hMADS cell adipogenesis

Previous in vitro enzymatic assays using human recombinant proteins showed that aldose reductase-B1 had PGF synthase activity whereas B10 isoform was completely devoid of such activity (22). Therefore, we evaluated the functional link between *AKR1B1* expression and $PGF_{2\alpha}$ production during adipogenic differentiation of hMADS cells. Under differentiation conditions, $PGF_{2\alpha}$ production rate of flow from hMADS cells increased progressively throughout adipogenesis to reach a 3-fold induction in mature hMADS adipocytes at day 15 (Figure 4A). This increase in $PGF_{2\alpha}$ output was tightly correlated with changes in *AKR1B1* expression at both mRNA and protein levels (Figures 3A and 4A and Supplemental Figure 4B) and independent from changes in the gene expression of other PGF synthases, ie, *AKR1A1* and *AKR1C3* (Figure 3A). Consistent with the observations from mouse 3T3-L1 cells, expression of the rate-limiting enzymes COX was either constitutive (COX-1) or inhibited (COX-2) upon induction of differentiation and remained very low during hMADS cell adipogenesis (Figure 4B).

As shown in Figure 4B, expression of both FP_A and FP_B isoforms of $PGF_{2\alpha}$ receptor was maximal in proliferative preadipocytes (day -3). It then decreased dramatically after day 3 (FP_A, 17% of day -3 value) or day 6 (FP_B, 6% of day -3 value) and remained low in maturing adipocytes. This suggested that $PGF_{2\alpha}$ released by adipocytes may essentially exert its antiadipogenic action in undifferentiated hMADS cells. Soon after differentiation commitment, FP receptors were turned off to trigger the adipogenic program and maintained at low levels throughout terminal differentiation. These low but detectable amounts of FP proteins coexisting with high $PGF_{2\alpha}$ levels would imply that $PGF_{2\alpha}$ could also have some function in mature adipocytes.

Exposure of hMADS cells to the specific aldose reductase inhibitor Statil (Ponalrestat) over the 2-week differentiation period resulted in an 18% reduction in cumulative $PGF_{2\alpha}$ production (Figure 4C). Remaining $PGF_{2\alpha}$ accumulation could be attributed to constant expression of *AKR1A1* or *AKR1C3* (Figure 3A) whose PGF synthase activities are insensitive to Statil (38). The ability of hMADS cells to accumulate intracellular lipids when exposed to adipogenic medium in the absence or presence of Statil was then examined by Oil-Red-O staining. As shown in Figure 4D, lipid accumulation was significantly increased by Statil treatment. As expected, Statil had no effect per se on *AKR1B1*, *A1*, *B10*, or *C3* gene expression (Figure 4E). We thus concluded that increased $PGF_{2\alpha}$ release during hMADS adipogenesis was partially associated with aldose reductase-B1 activity that might contribute to delay adipocyte differentiation.

Interestingly, the reduction in $PGF_{2\alpha}$ production resulting from hMADS Statil treatment led to a concomitant decrease in *COX-2/PTGS 2* expression (Figure 4E), whereas *COX-1* was unaltered (not shown). This observation was in agreement with previous demonstration of a $PGF_{2\alpha}$-dependent up-regulation of *COX-2* gene in 3T3-L1 cells (42). Our data thus confirm such a positive feedback loop for $PGF_{2\alpha}$ in human adipocytes.

Role of aldose reductase-dependent $PGF_{2\alpha}$ production on the adipogenic program

Our kinetics expression data underscored the main changes occurring during the first 3 days of differentiation for most of the actors involved in $PGF_{2\alpha}$ production/response. Further experiments were conducted to evaluate the effect of Statil over the first 3 days of differentiation and the impact of aldose reductase-dependent $PGF_{2\alpha}$ production during this critical period (Figure 5). Compared with the vehicle condition, 10 μM Statil treatment resulted in a 27% decrease in $PGF_{2\alpha}$ release associated with a concomitant increase in the expression of the transcripts for proadipogenic regulators *C/EBP*β and *C/EBP*α and for adipocyte marker *ATGL*, the lipolytic adipose triglyceride lipase. As expected, this treatment had no effect on *AKR* genes or on *COX-1* expression and was too brief to alter *COX-2* mRNA levels (not shown). To evaluate the ability of $PGF_{2\alpha}$ to reverse the Statil-dependent increase in adipose conversion, hMADS cells cultured in adipogenic medium for 6 days were concomitantly exposed to the FP agonist cloprostenol in the presence of Statil. As shown in Figure 5, C and D, cloprostenol exposure counteracted Statil effects on both intracellular lipid accumulation and expression of transcripts for proadipogenic factors *C/EBP*α and *PPAR*γ. Altogether our data indicate that, in hMADS cells, Statil exerts a primary proadipogenic effect at least by inhibiting aldose reductase-dependent $PGF_{2\alpha}$ synthesis.

Discussion

Previous data showing that certain aldose reductases are endowed with genuine $PGF_{2\alpha}$ synthase activity has pro-

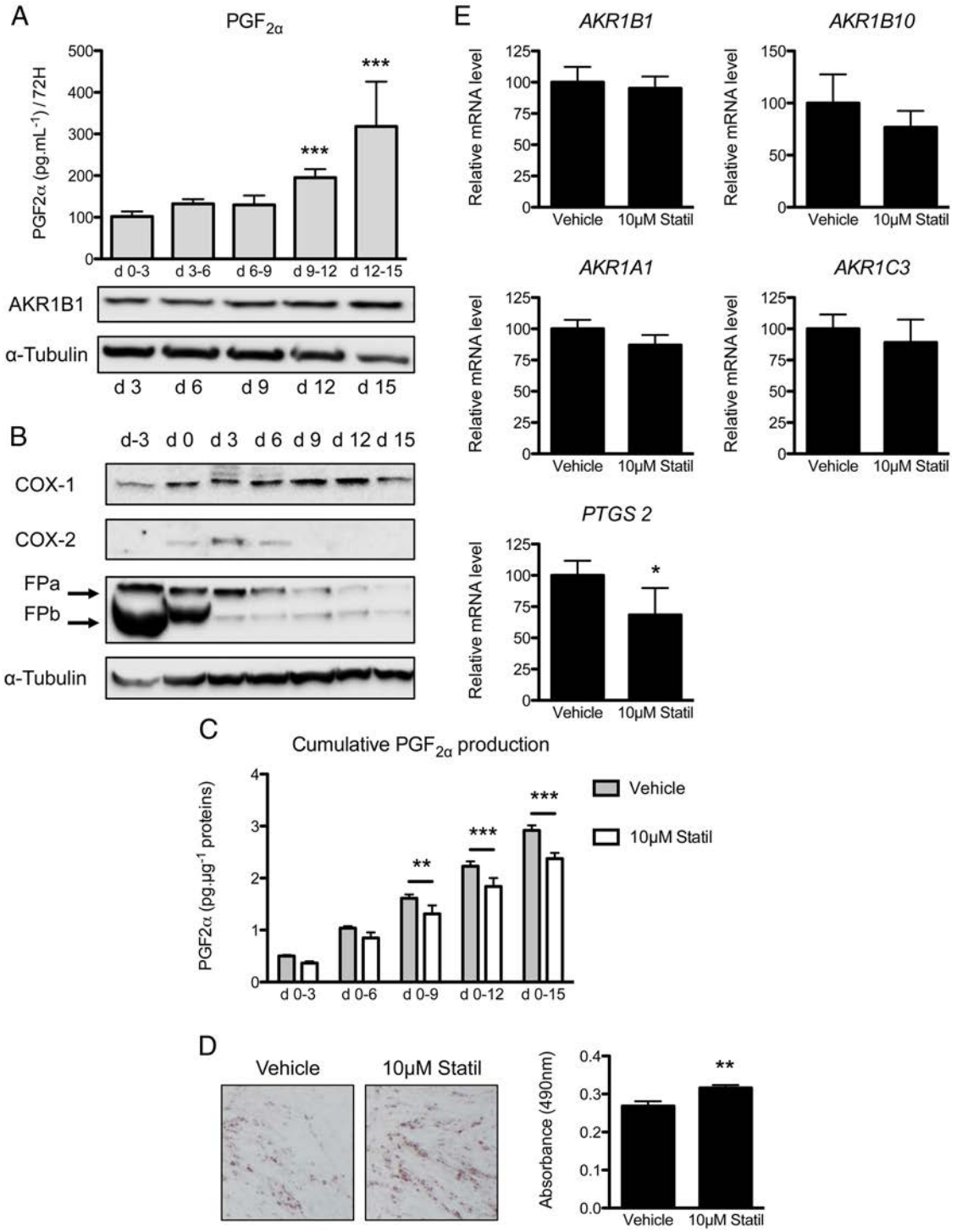

Figure 4. $PGF_{2\alpha}$ flow is correlated to *AKR1B1* expression during hMADS cell adipogenesis and is sensitive to Statil inhibitor. A, Culture media were collected every 3 days from day 0 to day 15 during hMADS cell differentiation and levels of released $PGF_{2\alpha}$ were determined by EIA. AKR1B1 protein was detected by Western blot in hMADS cells extracts. α-Tubulin was used as a loading control. B, COX-1, COX-2, FP_A, and FP_B accumulation were analyzed by Western blot during hMADS differentiation. α-Tubulin was used as a loading control. C, Effects of aldose reductase Statil inhibitor on cumulative $PGF_{2\alpha}$ production of hMADS cells. hMADS cells were treated with Statil or DMSO (vehicle) during the entire 15-day differentiation period. Culture media were collected every 3 days and $PGF_{2\alpha}$ levels measured by EIA. D, hMADS cells were differentiated for 9 days in the absence (vehicle) or presence of 10 μM Statil, fixed, and stained for triglycerides with Oil-Red-O. To quantify staining, Oil-Red-O was extracted from differentiating adipocytes and absorbance was then measured at 490 nm. E, hMADS cells were differentiated during 15 days in the presence of Statil or DMSO (vehicle) and expression of *AKR1B1*, *AKR1B10*, *AKR1A1*, *AKR1C3*, and *PTGS 2* genes were analyzed by RT-qPCR, normalized to *TBP*, and expressed as a percentage of vehicle treatment values. Statistical analyses in panel A were performed by one-way ANOVA followed by a Dunnett's post hoc test. Statistical analyses in panel C were performed by a two-way ANOVA followed by a Bonferroni post hoc test. In panels D and E, statistical analyses were performed by an unpaired *t* test. *, $P < .05$; **, $P < .01$; ***, $P < .001$.

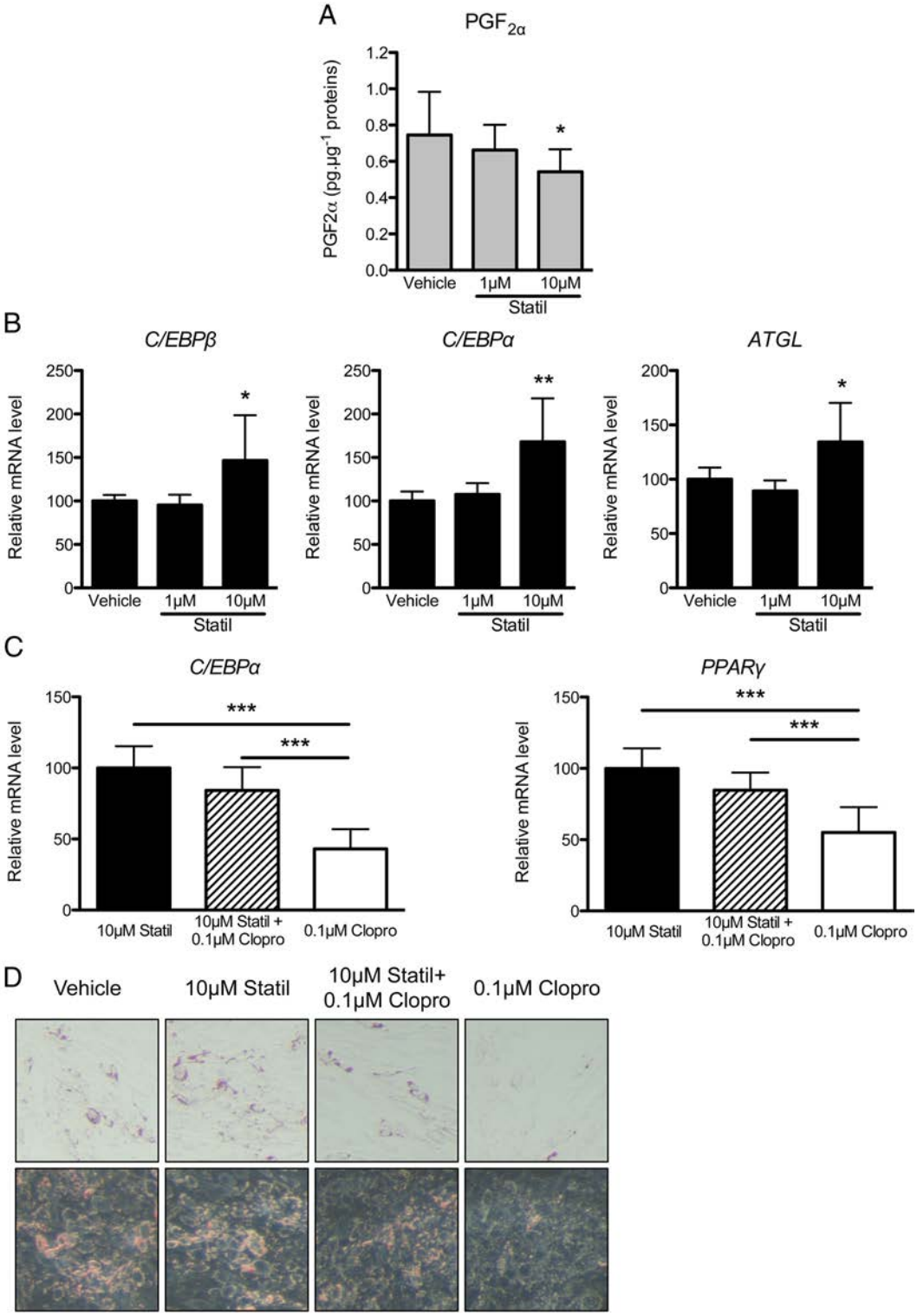

Figure 5. Statil enhances hMADS adipocyte differentiation by inhibiting aldose reductase-dependent $PGF_{2\alpha}$ synthesis. A, Effects of aldose reductase Statil inhibitor on $PGF_{2\alpha}$ release in culture media were determined by EIA in hMADS cells treated with Statil or its vehicle during the first 3 days of differentiation. B, mRNA levels of *C/EBPβ*, *C/EBPα*, and *ATGL* were monitored by RT-qPCR and normalized to *TBP*. Results were expressed as percentage of vehicle treatment values. C and D, Effects of Statil and cloprostenol ($PGF_{2\alpha}$ analog) treatments were examined after 6 days of differentiation on *C/EBPα* and *PPARγ* expression by RT-qPCR (C) and on intracellular lipid accumulation by Oil-Red-O staining (D; bright field and contrast phase views). Statistical analyses in panels A and B were performed by one-way ANOVA followed by a Dunnett's post hoc test, each value was compared with vehicle value. Statistical analyses in panel C were performed by a two-way ANOVA followed by a Bonferroni post hoc test. *, $P < .05$; **, $P < .01$, ***, $P < .001$.

vided the first evidence for their possible influence on endocrine or metabolic functions [(16, 22, 33); for review see reference 43]. More recently constitutive *Akr1b7* gene knockout in mice allowed the in vivo demonstration that decreased $PGF_{2\alpha}$ production resulting from aldose reductase-b7 loss could affect adipose tissue homeostasis without compensation by other related isoforms (23). Here we performed comparative and quantitative analysis of the expression of aldose reductase (*Akr1b* subfamily) genes in a set of mouse tissues with a focus on adipose depots and adipose tissue fractions. Our data highlighted the unique adipose-specific features of mouse aldose reductase-b7, in line with its antiadipogenic action in vivo and revealed that in humans aldose reductase-B1 isoform might also regulate adipogenic differentiation at least by a $PGF_{2\alpha}$-dependent mechanism.

Aldose reductase isoforms in adipose tissues: minor expression sites for a probable major physiological function

Although aldose reductase-b3 remains the most abundant isoform in mouse adipose tissues, our quantitative studies reveal that fat represents a common expression site for all aldose reductase-like genes (at least one of their top 5 tissues is adipose tissue, Table 2). Previous in vitro experiments have anticipated the possible impact of these proteins on adipose tissue homeostasis. We reported that aldose reductase-b7 had antiadipogenic action when overexpressed in 3T3-L1 preadipocytes (31). Although the underlying mechanisms were not elucidated at that time, later evidence that it was endowed with PGF synthase activity suggested that aldose reductase-b7-mediated $PGF_{2\alpha}$ production was likely to support inhibition of adipocyte differentiation (22, 33). This was definitively proven in vivo by using *Akr1b7* knockout mice that developed excessive adiposity in correlation with decreased accumulation of $PGF_{2\alpha}$ (23). In the meantime, it was shown that endogenous aldose reductase-b3 could also fulfill the $PGF_{2\alpha}$-dependent suppression of adipocyte differentiation in the T3-L1 cell line (24). Interestingly, these authors reported that *Akr1b3* expression was regulated throughout the 3T3-L1 differentiation program, mRNA levels showing a transient increase during the first day after the initiation of differentiation and then returning to low levels in maturing cells.

Although we broadly confirm these previous observations, we reveal herein that all aldose reductase genes (except *Akr1b16* that was constitutive) and to a lesser extent *Ptgfr* gene (encoding FP receptor) are differentially expressed during 3T3-L1 adipogenesis with transient and maximal mRNA levels coinciding with the onset of differentiation and decreasing thereafter. Moreover, this observation was confirmed at the protein levels, suggesting that their coordinated down-regulation could be required for completion of the adipogenic program. Although both aldose reductases-b3 and -b7 were reported to negatively regulate 3T3-L1 differentiation through PGF synthase activity, we show that endogenous aldose reductase-b7 amounts are very low compared with that of -b3 (Figure 2). Conversely, *Akr1b3* ablation in mice had no impact on adipose tissues, whereas loss of *Akr1b7* induced, as expected, an expansion of fat (23). Therefore, aldose reductases function in adipose tissue should be investigated in vivo as much as possible. Here we report in vivo characterization of *Akr1b* genes expression within the two functional fractions of fat depots, ie, adipocytes and SVF. These data underscore the unique signature of *Akr1b7* expression, which is the only gene of the four Akr1b genes in mouse to show a depot-specific pattern and absence of expression in mature adipocytes (Table 2 and Figure 1). *Akr1b3* shows higher expression in the adipocyte fraction, thus contrasting with 3T3-L1 data (Figure 2 and reference 24). Altogether these observations suggest that aldose reductase-b7 functions in WAT are not overlapped by other isoforms, which is in good agreement with the adipose phenotype of $Akr1b7^{-/-}$ mice. The identification of the cell population within SVF, which supports *Akr1b7* expression and relays its antiadipogenic action, is currently in progress.

Antiadipogenic action of aldose reductase-dependent $PGF_{2\alpha}$ production is conserved in humans

Aldose reductase-B1 isoform was shown to be expressed in primary preadipocytes isolated from human fat tissue, in close correlation with cytokine-induced $PGF_{2\alpha}$ release. However, its impact on adipogenesis remains unknown (26). Our study suggests that the mode of action of these enzymes on adipose tissue homeostasis could differ in human and mouse. Using multipotent cells isolated from human adipose tissue (hMADS line), we show that expression of *AKR1B1*, the human homolog of mouse *Akr1b3*, parallels hMADS adipogenic differentiation in close correlation with $PGF_{2\alpha}$ release. Importantly, we demonstrate that inhibition of $PGF_{2\alpha}$ production using a specific aldose reductase inhibitor (Statil) during hMADS adipogenesis enhances adipocyte differentiation, whereas exogenous $PGF_{2\alpha}$ counteracts Statil effects (Figure 5). Hence, in human as in mouse, the aldose reductase-dependent production of $PGF_{2\alpha}$ might participate in restricting differentiation of preadipocytes in a cell autonomous manner but the means of this restriction may differ. Unlike *Akr1b3* in 3T3-L1, the expression of *AKR1B1* is not down-regulated but steadily increases throughout adipo-

genesis. However, $PGF_{2\alpha}$ receptors expression is turned down after day 3 of hMADS differentiation (compare Figures 2 and 4). This suggests that the need to overcome the repressive effect of $PGF_{2\alpha}$ on adipogenesis might be mainly achieved by limiting its signaling potential (by down-regulating FP receptors) in human cells and by limiting its synthesis (by down-regulating aldose reductase-b3 and -b7 PGF synthases) in mouse preadipocytes. Nevertheless, we show that in both species, genes encoding aldose reductase-like devoid of PGF synthase activity, ie, *Akr1b8* and *AKR1B10* show maximum mRNA accumulation in undifferentiated adipocytes and are down-regulated in maturing adipocytes (Figures 2 and 3*A*).

In terms of structural conservations, substrate spectra and tissue distribution, murine aldose reductase-b8 is considered as the ortholog of human aldose reductase-B10 (44). In addition to $PGF_{2\alpha}$, other signaling molecules such as those produced by the vitamin A (retinol) metabolism, retinoic acid and retinaldehyde (Rald) are known to negatively regulate adipogenesis (45, 46). Interestingly both aldose reductase-B10 and aldehyde reductase-C3 display the best Rald reductase activity among aldose and aldehyde reductases (for review see reference 47). Once synthesized, Rald concentration depends both on its rate of irreversible oxidation to retinoic acid and on its rate of reduction back to retinol. Although we showed that *Akr1b8/AKR1B10* and *AKR1C3* are differentially expressed after adipogenic stimulation, further experiments will be needed to unravel the possible impact of these genes as regulators of adipogenesis by influencing retinoid metabolism.

Taken together, our findings establish aldose reductases as previously unrecognized contributors of adipose tissue homeostasis. By comparing human and mouse isoforms in preadipocyte culture models, we propose that the two species have developed different but convergent strategies to control $PGF_{2\alpha}$ production and its biological impact on fine-tuning early adipocyte differentiation. Finally, our findings establish the background for further evaluation of pharmacological aldose reductase inhibitors, initially designed to treat diabetic complications, as potential obesogenic compounds.

Acknowledgments

We thank all the members of the team for helpful discussions. We also thank Sandrine Plantade, Khirredine Ouchen, and Philippe Mazuel for excellent animal care.

Address all correspondence and requests for reprints to: Anne-Marie Lefrançois-Martinez and Antoine Martinez, Centre National de la Recherche Scientifique Unité Mixte de Recherche 6293, INSERM Unité 1103, Génétique Reproduction and Développement, Clermont Université, BP80026, 24 Avenue des Landais, 63171 Aubière Cedex, France. E-mail: a-marie.lefrancois-martinez@univ-bpclermont.fr; or antoine.martinez@univ-bpclermont.fr.

This work was supported by the Université Blaise Pascal, the Université d'Auvergne, the Centre National de la Recherche Scientifique, Institut National de la Santé et de la Recherche Médicale and by a grant from the Conseil Régional d'Auvergne Contrat de Plan Etat Région/Fonds Européens de Développement Régional 2010 Laboratoire d'Excellence and a PhD grant from the Société Française d'Endocrinologie.

Disclosure Summary: The authors have nothing to disclose.

References

1. **Bohren KM, Bullock B, Wermuth B, Gabbay KH.** The aldo-keto reductase superfamily. cDNAs and deduced amino acid sequences of human aldehyde and aldose reductases. *J Biol Chem*. 1989;264(16):9547–9551.
2. **Cao D, Fan ST, Chung SS.** Identification and characterization of a novel human aldose reductase-like gene. *J Biol Chem*. 1998;273(19):11429–11435.
3. **Hyndman DJ, Flynn TG.** Sequence and expression levels in human tissues of a new member of the aldo-keto reductase family. *Biochim Biophys Acta*. 1998;1399(2–3):198–202.
4. **Salabei JK, Li X-P, Petrash JM, Bhatnagar A, Barski OA.** Functional expression of novel human and murine AKR1B genes. *Chem Biol Interact*. 2011;191(1–3):177–184.
5. **Gui T, Tanimoto T, Kokai Y, Nishimura C.** Presence of a closely related subgroup in the aldo-keto reductase family of the mouse. *Eur J Biochem*. 1995;227(1–2):448–453.
6. **Pailhoux EA, Martinez A, Veyssiere GM, Jean CG.** Androgen-dependent protein from mouse vas deferens. cDNA cloning and protein homology with the aldo-keto reductase superfamily. *J Biol Chem*. 1990;265(32):19932–19936.
7. **Donohue PJ, Alberts GF, Hampton BS, Winkles JA.** A delayed-early gene activated by fibroblast growth factor-1 encodes a protein related to aldose reductase. *J Biol Chem*. 1994;269(11):8604–8609.
8. **Fukumoto S-I, Yamauchi N, Moriguchi H, et al.** Overexpression of the aldo-keto reductase family protein AKR1B10 is highly correlated with smokers' non-small cell lung carcinomas. *Clin Cancer Res*. 2005;11(5):1776–1785.
9. **Woenckhaus M, Klein-Hitpass L, Grepmeier U, et al.** Smoking and cancer-related gene expression in bronchial epithelium and non-small-cell lung cancers. *J Pathol*. 2006;210(2):192–204.
10. **Heringlake S, Hofdmann M, Fiebeler A, Manns MP, Schmiegel W, Tannapfel A.** Identification and expression analysis of the aldo-ketoreductase1–B10 gene in primary malignant liver tumours. *J Hepatol*. 2010;52(2):220–227.
11. **Kang MW, Lee ES, Yoon SY, et al.** AKR1B10 is associated with smoking and smoking-related non-small-cell lung cancer. *J Int Med Res*. 2011;39(1):78–85.
12. **Schmitz KJ, Sotiropoulos GC, Baba HA, et al.** AKR1B10 expression is associated with less aggressive hepatocellular carcinoma: a clinicopathological study of 168 cases. *Liver Int*. 2011;31(6):810–816.
13. **Yadav UCS, Srivastava SK, Ramana KV.** Aldose reductase inhibition prevents endotoxin-induced uveitis in rats. *Invest Ophthalmol Vis Sci*. 2007;48(10):4634–4642.
14. **Yadav UCS, Ramana KV, Aguilera-Aguirre L, Boldogh I, Boulares HA, Srivastava SK.** Inhibition of aldose reductase prevents experimental allergic airway inflammation in mice. Hartl D, ed. *PLoS ONE*. 2009;4(8):e6535.
15. **Yadav UCS, Shoeb M, Srivastava SK, Ramana KV.** Aldose reductase

deficiency protects from autoimmune- and endotoxin-induced uveitis in mice. *Invest Ophthalmol Vis Sci.* 2011;52(11):8076–8085.
16. **Bresson E, Boucher-Kovalik S, Chapdelaine P, et al.** The human aldose reductase AKR1B1 qualifies as the primary prostaglandin F synthase in the endometrium. *J Clin Endocrinol Metab*. 2011;96(1): 210–219.
17. **Barski OA, Tipparaju SM, Bhatnagar A.** The aldo-keto reductase superfamily and its role in drug metabolism and detoxification. *Drug Metab Rev*. 2008;40(4):553–624.
18. **Ramana KV, Yadav UCS, Calhoun WJ, Srivastava SK.** Current prospective of aldose reductase inhibition in the therapy of allergic airway inflammation in asthma. *Curr Mol Med*. 2011;11(7):599–608.
19. **Srivastava SK, Ramana KV, Bhatnagar A.** Role of Aldose Reductase and Oxidative Damage in Diabetes and the Consequent Potential for Therapeutic Options. *Endocrine Reviews*. 2005;26(3):380–392. doi:10.1210/er.2004–0028.
20. **Reginato MJ, Krakow SL, Bailey ST, Lazar MA.** Prostaglandins promote and block adipogenesis through opposing effects on peroxisome proliferator-activated receptor gamma. *J Biol Chem*. 1998; 273(4):1855–1858.
21. **Liu L, Clipstone NA.** Prostaglandin F2α inhibits adipocyte differentiation via a Gαq-calcium-calcineurin-dependent signaling pathway. *J Cell Biochem*. 2007;100(1):161–173.
22. **Kabututu Z, Manin M, Pointud J-C, et al.** Prostaglandin F2α synthase activities of aldo-keto reductase 1B1, 1B3 and 1B7. *J Biochem*. 2009;145(2):161–168.
23. **Volat FE, Pointud J-C, Pastel E, et al.** Depressed levels of prostaglandin F2α in mice lacking Akr1b7 increase basal adiposity and predispose to diet-induced obesity. *Diabetes*. 2012;61(11):2796–2806.
24. **Fujimori K, Ueno T, Nagata N, et al.** Suppression of adipocyte differentiation by aldo-keto reductase 1B3 acting as prostaglandin F2α synthase. *J Biol Chem*. 2010;285(12):8880–8886.
25. **Baba SP, Hellmann J, Srivastava S, Bhatnagar A.** Aldose reductase (AKR1B3) regulates the accumulation of advanced glycosylation end products (AGEs) and the expression of AGE receptor (RAGE). *Chem Biol Interact*. 2011:1–7.
26. **Michaud A, Lacroix-Pépin N, Pelletier M, et al.** Prostaglandin (PG) F2α synthesis in human subcutaneous and omental adipose tissue: modulation by inflammatory cytokines and role of the human aldose reductase AKR1B1. *PLoS One*. 2014;9(3):e90861.
27. **Student AK, Hsu RY, Lane MD.** Induction of fatty acid synthetase synthesis in differentiating 3T3-L1 preadipocytes. *J Biol Chem*. 1980;255(10):4745–4750.
28. **Rodriguez AM, Elabd C, Amri E-Z, Ailhaud G, Dani C.** The human adipose tissue is a source of multipotent stem cells. *Biochimie*. 2005; 87(1):125–128.
29. **Zaragosi L-E, Ailhaud G, Dani C.** Autocrine fibroblast growth factor 2 signaling is critical for self-renewal of human multipotent adipose-derived stem cells. *Stem Cells*. 2006;24(11):2412–2419.
30. **Mohsen-Kanson T, Hafner A-L, Wdziekonski B, et al.** Differentiation of human induced pluripotent stem cells into brown and white adipocytes: role of Pax3. *Stem Cells*. 2014;32(6):1459–1467.
31. **Tirard J, Gout J, Lefrançois-Martinez A-M, Martinez A, Begeot M, Naville D.** A novel inhibitory protein in adipose tissue, the aldo-keto reductase AKR1B7: its role in adipogenesis. *Endocrinology*. 2007; 148(5):1996–2005.
32. **Pfaffl MW.** *A-Z of Quantitative PCR*. La Jolla, CA: SA Bustin; 2004:87–112.
33. **Lambert-Langlais S, Pointud J-C, Lefrançois-Martinez A-M, et al.** Aldo keto reductase 1B7 and prostaglandin F2α are regulators of adrenal endocrine functions. Vella A, ed. *PLoS One*. 2009;4(10): e7309.
34. **Cawthorn WP, Scheller EL, MacDougald OA.** Adipose tissue stem cells meet preadipocyte commitment: going back to the future. *J Lipid Res*. 2012;53(2):227–246.
35. **Yan H, Kermouni A, Abdel-Hafez M, Lau DCW.** Role of cyclooxygenases COX-1 and COX-2 in modulating adipogenesis in 3T3-L1 cells. *J Lipid Res*. 2003;44(2):424–429.
36. **Lu S, Nishimura K, Hossain MA, Jisaka M, Nagaya T, Yokota K.** Regulation and role of arachidonate cascade during changes in life cycle of adipocytes. *Appl Biochem Biotechnol*. 2004;118(1–3):133–153.
37. **Komoto J, Yamada T, Watanabe K, Takusagawa F.** Crystal structure of human prostaglandin F synthase (AKR1C3). *Biochemistry*. 2004;43(8):2188–2198.
38. **Pépin NL, Chapdelaine P, Fortier MA.** Evaluation of the prostaglandin F synthase activity of human and bovine aldo-keto reductases: AKR1A1s complement AKR1B1s as potent PGF synthases. *Prostagland Other Lipid Mediat*. 2013:1–9.
39. **Ma J, Yan R, Zu X, et al.** Aldo-keto reductase family 1 B10 affects fatty acid synthesis by regulating the stability of acetyl-CoA carboxylase-alpha in breast cancer cells. *J Biol Chem*. 2008;283(6): 3418–3423.
40. **Rodriguez A-M, Elabd C, Delteil F, et al.** Adipocyte differentiation of multipotent cells established from human adipose tissue. *Biochem Biophys Res Commun*. 2004;315(2):255–263.
41. **Kang S, Akerblad P, Kiviranta R, et al.** Regulation of early adipose commitment by Zfp521. Vidal-Puig AJ, ed. *PLoS Biol*. 2012;10(11): e1001433.
42. **Fujimori K, Yano M, Ueno T.** Synergistic suppression of early phase of adipogenesis by microsomal PGE synthase-1 (PTGES1)-produced PGE2 and aldo-keto reductase 1B3-produced PGF2α. Giorgino F, ed. *PLoS One*. 2012;7(9):e44698.
43. **Pastel E, Pointud J-C, Volat F, Martinez A, Lefrançois-Martinez A-M.** Aldo-keto reductases 1B in endocrinology and metabolism. *Front Pharmacol*. 2012;3:148.
44. **Joshi A, Rajput S, Wang C, Ma J, Cao D.** Murine aldo-keto reductase family 1 subfamily B: identification of AKR1B8 as an ortholog of human AKR1B10. *Biol Chem*. 2010;391(12):1371–1378.
45. **Xue JC, Schwarz EJ, Chawla A, Lazar MA.** Distinct stages in adipogenesis revealed by retinoid inhibition of differentiation after induction of PPARγ. *Mol Cell Biol*. 1996;16(4):1567–1575.
46. **Ziouzenkova O, Orasanu G, Sharlach M, et al.** Retinaldehyde represses adipogenesis and diet-induced obesity. *Nat Med*. 2007; 13(6):695–702.
47. **Ruiz FX, Porté S, Parés X, Farrés J.** Biological role of aldo-keto reductases in retinoic acid biosynthesis and signaling. *Front Pharmacol*. 2012;3:58.